Mon. Not. R. Astron. Soc. **000**, 1–12 (2004) Printed 2 February 2008 (MN LATEX style file v2.2)

Simulating Galaxy Clusters - III: Properties of the Intracluster Stars

Jesper Sommer-Larsen[1,2,3⋆], Alessio D. Romeo[1,2,4]† and Laura Portinari[1,5]‡
[1] *Theoretical Astrophysics Center, Juliane Maries Vej 30, DK-2100 Copenhagen, Denmark*
[2] *Nordita, Blegdamsvej 17, DK-2100 Copenhagen, Denmark*
[3] *Astronomical Observatory, University of Copenhagen, Juliane Maries Vej 30, 2100 Copenhagen Ø, Denmark*
[4] *Dipartimento di Fisica e Astronomia, Università di Catania, via S.Sofia 64, 95123 Catania, Italy*
[5] *Tuorla Observatory, Väisäläntie 20, FIN-21500 Piikkiö, Finland*

Accepted —. Received —; in original form 2004 March 11

ABSTRACT

Cosmological (ΛCDM) TreeSPH simulations of the formation and evolution of galaxy groups and clusters have been performed. The simulations invoke star formation, chemical evolution with non-instantaneous recycling, metallicity dependent radiative cooling, strong star-burst, and (optionally) AGN, driven galactic super-winds, effects of a meta-galactic UV field and thermal conduction. Results for two clusters, one Virgo-like ($T\simeq$3 keV) and one (sub) Coma-like ($T\simeq$6 keV), are presented. At z=0 the stellar contents of both clusters consist of a central dominant (cD) galaxy surrounded by cluster galaxies and intracluster stars. The intracluster (IC) stars are found to contribute 20-40% of the total cluster B-band luminosity at z=0 and to form at a mean redshift $\bar{z}_f \sim$3 being on average about 0.5 Gyr older than the stars in cluster galaxies. UBVRIJHK surface brightness profiles of the IC star populations are presented; the profile of the larger cluster matches the observed V-band profile of the cD in Abell 1413 ($T \simeq$8 keV) quite well. The typical colour of the IC stellar population is B-R=1.4-1.5, comparable to the colour of sub-L^* E and S0 galaxies. The mean Iron abundance of the IC stars is about solar in the central part of the cluster ($r \sim$100 kpc) decreasing to about half solar at the virial radius. The IC stars are α-element enhanced with a weak trend of [O/Fe] increasing with r and an overall [O/Fe]$\sim$0.4 dex, indicative of dominant enrichment from type II supernovæ.

The IC stars are kinematically significantly colder than the cluster galaxies: The velocity dispersions of the IC stars are in the inner parts of the clusters ($r \sim$100-500 kpc) only about half of those of the cluster galaxies increasing slightly outward to about 70% at r=1-2 Mpc. The typical projected velocity dispersion in the Virgo-like cluster at $R \gtrsim 50$ kpc is 300-600 km/s depending on orientation and projected distance from the cluster center. Rotation is found to be dynamically insignificant for the IC stars. The velocity distributions of IC stars *and* clusters galaxies are in one cluster highly radially anisotropic, in the other close to isotropic.

Key words: cosmology: theory — cosmology: numerical simulations — galaxies: clusters — galaxies: formation — galaxies: evolution

1 INTRODUCTION

Current hierarchical or "bottom-up" structure formation theories predict that the field star populations of haloes of galaxies like the Milky Way should consist partly of stars originally born in small proto-galaxies and later tidally stripped from these by the main galaxy or through interaction with other proto-galaxies. The fraction of halo field stars of such origin depends (apart from obvious cosmic variance effects) on the properties of the dark matter (e.g., cold dark matter, CDM, vs. warm dark matter, WDM: for WDM the hierarchy is broken at the free-streaming mass scale, e.g., Sommer-Larsen & Dolgov 2001) and the nature of the star-formation process. For example, some halo stars may be born in rapidly expanding, supernova driven proto-galactic supershells and hence be detached from their parent proto-

⋆ E-mail: jslarsen@tac.dk
† E-mail: aro@ct.astro.it
‡ E-mail: lporti@utu.fi

galaxies right from the outset in space, as well as phase-space (e.g., Mori et al. 1997; Sommer-Larsen, Götz & Portinari 2003). If dark matter is cold and star-formation in expanding supershells is not a common phenomenon the above fraction could be quite large, in principle at least, approaching unity (e.g., Helmi et al. 2003). The halo stars resulting from tidal stripping or disruption of a proto-galaxy will stay localized in phase-space for a long period and several such "streams" of halo stars have been detected in the haloes of the Milky Way and M31 (e.g., Helmi et al. 1999; Ferguson et al. 2002).

From the point of view of structure formation, galaxy clusters can be seen as scaled up versions of galaxies in hierarchical scenarios. In particular, gravity is expected to strip or disrupt cluster galaxies in a similar way as satellite galaxies in galaxy haloes and a population of intracluster (or "field") stars should thus reside between the cluster galaxies. It has been known for decades that cD galaxies often are embedded in extended envelopes presumed to consist of stars tidally stripped off galaxies in the process of being engulfed by the cD (e.g., Oemler 1976; Dressler 1979). In recent years it has been possible to perform quantitative studies of these stellar envelopes through ultra-deep surface photometry of the general stellar population (e.g., Gonzalez et al. 2000; Gonzalez, Zabludoff & Zaritsky 2004; Feldmeier et al. 2002, 2004a), or imaging/spectroscopy of individual planetary nebulae (e.g., Arnaboldi et al. 2002, 2003; Feldmeier et al. 2004b) or supernovae Type Ia (Gal-Yam et al. 2003). The potential importance of intracluster stars in relation to the chemical enrichment of the intracluster medium (ICM) was recently discussed by Zaritsky, Gonzalez & Zabludoff (2004) and Lin & Mohr (2004).

On the theoretical front Napolitano et al. (2003) have used an N-body dark matter only fully cosmological simulation of the formation of a Virgo-like cluster to make predictions about intracluster stars. They find that unrelaxed velocity distributions and (bulk) streaming motions of the IC stars should be common due to the large dynamical timescales in clusters. Hence the evolution towards a relaxed coarse-grained phase-space distribution function through phase-mixing has proceeded much less far[1] than, e.g., in the Galactic halo, where dynamical timescales are much shorter.

The dark matter only simulations are complemented by various N-body simulations which invoke a more realistic modelling of the stellar properties of galaxies in order to study the fate of galaxies in a cluster environment (e.g., "galaxy harassment", Moore et al. 1996, "tidal stirring", Mayer et al. 2001 and the formation of the central cluster galaxy, Dubinski 1998). The advantage of this approach is that a very high resolution in the stellar component can be obtained. In relation to the properties of the IC stars, recent progress has been made by Dubinski et al. (2003), and Feldmeier et al. (2004a).

In general the properties of the system of IC stars are set by two main effects: a) the cool-out of gas and subsequent conversion of cold, high-density gas to stars in individual galaxies and b) the stripping/disruption of the galaxies through interactions with other galaxies and the main cluster potential. Since such interactions will generally affect the star-formation rate (as long as a reservoir of gas is available) the former process is intimately coupled to the latter.

Only fairly recently has it been possible to carry out fully cosmological gas-dynamical/N-body simulations of the formation and evolution of galaxy clusters at a sufficient level of numerical resolution and physical sophistication that the cool-out of gas, star-formation, chemical evolution and gas inflows and outflows related to individual cluster galaxies can be modelled to, at least some, degree of realism (e.g., Valdarnini 2003; Tornatore et al. 2004). Recently Murante et al. (2004) analyzed 117 clusters formed in a large cosmological TreeSPH simulation (Borgani et al. 2004) to study the properties of the IC stars. They determined average density profiles of the IC stars as well as stars in galaxies for their large sample of clusters. One of the interesting conclusions reached is that only at fairly large cluster-centric distances ($r \gtrsim 0.4$-$0.5 r_{\rm vir}$) does the (spherically averaged) density of stars in galaxies (excluding the cD) exceed that of IC stars. Complementary work has recently been performed by Willman et al. (2004), who simulated a Coma-like cluster at very high numerical resolution. They find an IC star fraction of 10-20%, in good agreement with observations, and a tendency for the fraction to increase with time. In relation to on-going observational efforts, they moreover find that line-of-sight velocities of intra-cluster planetary nebulae can be used for fairly accurate cluster mass estimation, even for dynamically quite unrelaxed clusters, if more than 5 fields at a range of projected radii are covered.

We have recently undertaken similar simulations of galaxy groups and clusters. We are building on our TreeSPH code used for simulating galaxy formation (e.g., Sommer-Larsen, Götz & Portinari 2003), improved to include modelling of non-instantaneous chemical evolution (Lia, Portinari & Carraro 2002a), metallicity-dependent, atomic radiative cooling, strong supernova, and (optionally) AGN, driven galactic winds and thermal conduction. The main results of the simulations concerning the properties of the ICM and cluster scaling relations are described in Paper I (Romeo et al. 2004), while the characteristics of the population of the simulated cluster galaxies are presented in Paper II (Romeo, Portinari & Sommer-Larsen 2004) — in this Paper III of the series, we discuss our first results on the properties of the IC stars in two simulated clusters, with masses and temperatures similar to the Virgo and Coma clusters, respectively. Our results complement those of Murante et al. (2004) and Willman et al. (2004), since we present for the IC stars also results on self-consistently calculated multiband surface brightness profiles, colours, abundances and detailed kinematics (Willman et al. 2004 also present a kinematics study, which we compare to in this paper).

In section 2 we briefly describe the code and the numerical simulations, in section 3 we present and discuss the results obtained, and finally section 4 constitutes our conclusions.

2 THE CODE AND SIMULATIONS

The code used for the simulations is a significantly improved version of the TreeSPH code we have used previously for galaxy formation simulations (Sommer-Larsen, Götz &

[1] A visualized example from one of our simulations is given at http://www.tac.dk/~jslarsen/ICstars

Portinari 2003): Full details on the code are given in Paper I, here we recall the main improvements over the previous version. (1) In lower resolution regions (which will always be present in cosmological CDM simulations) an improvement in the numerical accuracy of the integration of the basic equations is obtained by solving the entropy equation rather than the thermal energy equation — we have adopted the "conservative" entropy equation solving scheme suggested by Springel & Hernquist (2002). (2) Cold high-density gas is turned into stars in a probabilistic way as described in Sommer-Larsen, Götz & Portinari (2003). In a star-formation event an SPH particle is converted fully into a star particle. Non-instantaneous recycling of gas and heavy elements is described through probabilistic "decay" of star particles back to SPH particles as discussed by Lia, Portinari & Carraro (2002a). In a decay event a star particle is converted fully into an SPH particle. (3) Non-instantaneous chemical evolution tracing 10 elements (H, He, C, N, O, Mg, Si, S, Ca and Fe) has been incorporated in the code following Lia et al. (2002a,b); the algorithm includes supernovæ of type II and type Ia, and mass loss from stars of all masses. Metal diffusion in Lia et al. was included with a diffusion coefficient κ derived from models of the expansion of individual supernova remnants. A much more important effect in the present simulations, however, is the redistribution of metals (and gas) by means of star-burst driven "galactic super–winds" (see point 5). This is handled self-consistently by the code, so we set κ=0 in the present simulations. (4) Atomic radiative cooling depending both on the metal abundance of the gas and on the meta–galactic UV field, modelled after Haardt & Madau (1996) is invoked. We also include a simplified treatment of radiative transfer, by switching off the UV field where the gas becomes optically think to Lyman limit photons on scales of $\sim$ 1 kpc. (5) Star-burst driven, galactic super-winds are incorporated in the simulations. This is required to expel metals from the galaxies and get the abundance of the ICM to the observed level of about 1/3 solar in iron. A burst of star formation is modelled in the same way as the "early bursts" of Sommer-Larsen, Götz & Portinari (2003), i.e. by halting cooling in the surrounding gas particles, to mimic the initial heating and subsequent adiabatic expansion phase of the supershell powered by the star-burst; this scheme ensures effective energy coupling and feedback between the bursting star particle and the surrounding gas. The strength of the super-winds is modelled through a free parameter $f_{\rm wind}$ which determines how large a fraction of the new–born stars partake in such bursting, super-wind driving star formation. We find that in order to get an iron abundance in the ICM comparable to observations, $f_{\rm wind} \gtrsim 0.5$ and at the same time a fairly top-heavy Initial Mass Function (IMF) has to be used. (6) Thermal conduction was implemented in the code following Cleary & Monaghan (1999).

We ran simulations of two small and two larger galaxy groups as well as a Virgo-like and a (mini) Coma-like cluster — we shall denote the latter two clusters C1 and C2 in the following. All 6 systems were chosen to be fairly relaxed (no $\gtrsim$1:2 merging at $z \lesssim 1$). Virial masses at z=0 were approximately 3.4x10^{13}, 7.9x10^{13}, 2.0x10^{14} and 8.4x10^{14} h^{-1}M$_\odot$ and X-ray emission weighted temperatures 1.1, 1.6, 3.0 and 6.0 keV, respectively. The groups and clusters were selected from a cosmological, DM-only simulation of a flat ΛCDM model, with Ω_M=0.3, Ω_b=0.036, h=0.7 and σ_8=0.9 and a box-length of 150 h^{-1}Mpc. Mass and force resolution was increased in Lagrangian regions enclosing the groups and clusters, such that $m_{\rm gas}$=m_*= 2.5x10^8 and $m_{\rm DM}$=1.8x10^9 h^{-1}M$_\odot$ for the high resolution gas, star and dark matter particles. Particle numbers are in the range 100000-500000 baryonic+DM particles. Gravitational (spline) softening lengths of $\epsilon_{\rm gas}$=ϵ_*=2.8 and $\epsilon_{\rm DM}$=5.4 h^{-1}kpc, respectively, were adopted. The gravity softening lengths were fixed in physical coordinates from z=6 to z=0 and in comoving coordinates at earlier times. To test for numerical resolution effects one simulation was run with eight times higher mass resolution and two times higher force resolution, yielding $m_{\rm gas}$=m_*= 3.1x10^7 and $m_{\rm DM}$=2.3x10^8 h^{-1}M$_\odot$ and gravity softening lengths of 1.4 and 2.7 h^{-1}kpc, respectively.

For the simulation presented in this paper $f_{\rm wind}$=0.8, and an Arimoto-Yoshii IMF (of slope x=–1, shallower than the Salpeter slope x=-1.35) with mass limits [0.1–100] $M_\odot$ was adopted. AGN driven winds were not invoked. Moreover, the thermal conductivity was set to zero assuming that thermal conduction in the ICM is highly suppressed by magnetic fields (e.g., Ettori & Fabian 2000); notice however that, in relation to the cluster galaxy populations and hence also IC stars, no significant difference is found between simulations with zero thermal conductivity and simulations invoking thermal conduction at 1/3 of the Spitzer level (Paper II).

3 RESULTS AND DISCUSSION

In this section we present and discuss results for clusters C1 and C2 run at our "standard" resolution. The resolution test discussed in Section 3.7 indicates that none of the following results concerning mass and luminosity fractions, mean ages, surface brightness profiles, colours, abundances, kinematics and density profiles of the IC stars change in any significant way with increased numerical resolution.

All results presented in the following refer to z=0, unless another epoch is explicitly specified. At z=0 1.2x10^4 and 2.3x10^4 star particles are located inside of $r_{\rm vir}$=1.3 and 2.0 h^{-1}Mpc of the clusters C1 and C2[2]. The corresponding mass in stars is 2.9x10^{12} and 5.6x10^{12} h^{-1}M$_\odot$ or a fraction of about 1% of the total virial mass (the stellar mass fraction is smaller for C2 than for C1 - we shall return to this below). In both clusters the stellar mass constitutes 14% of the total baryonic mass inside of the virial radius. In the following we shall refer to star particles simply as "stars".

When preparing the initial conditions for C2, due to computational limitations we sampled with split DM+SPH particles a region somewhat smaller than the "virial volume". The volume outside this region, but still inside of the virial volume, is represented by high resolution, DM-only particles (with a mass scaled by $1/(1-f_b)$ with respect to the DM particles in the inner DM+SPH region, since they are not

[2] In this paper the virial radius $r_{\rm vir}$ is the radius corresponding to, at z=0, an over-density 337 times the mean density of the Universe, as appropriate for a top–hat collapse in the adopted ΛCDM cosmology (e.g., Bryan & Norman 1998). The virial mass $M_{\rm vir}$ of the cluster is the mass enclosed within the region of radius $r_{\rm vir}$.

split into baryonic and DM component; f_b is the universal baryon fraction, assumed to be 0.12 in this work); finally, the region outside the virial volume is, as usual, sampled by lower resolution dark matter particles with masses increasing with distance from the virial volume. As a consequence of this baryonic under-sampling, about half of the mass inside of the virial radius of the final cluster is in the form of (high–resolution) DM-only particles, i.e. not split into SPH+DM. The relative percentage of these DM-only particles increases with radius, hence the amount of late infall of gas and galaxies is reduced compared to the fully resolved case. This explains why the stellar mass fraction in C2 is smaller than that in C1 as mentioned above (the C2 star mass is only about twice the C1 star mass, while the respective virial masses differ by a factor of about four). The ratio of the respective number of galaxies $N_{\rm gal}$(C2)/$N_{\rm gal}$(C1) is also smaller than the ratio of the corresponding virial masses (again, a factor of $\sim$2 vs. a factor of $\sim$4, see below) and the average ages of the IC stars and galaxies in C2 are slightly larger than that in C1, due to the under-sampling of late infall of galaxies at the outskirts (Section 3.3). Since the results we discuss refer to the inner 1–2 Mpc, the baryonic under-sampling of the outskirts is not a crucial problem. Moreover, we have initiated a simulation of C2 with full baryonic sampling of the virial volume; at a redshift of $z = 0.8$ this shows no significant difference in relation to the results on IC stars presented here.

The stellar contents of both clusters are characterized by a massive, central dominant (cD) galaxy surrounded by galaxies and intracluster stars. The effective radii, calculated from the B-band surface brightness profiles of the two cD galaxies, are $R_{eff} \simeq$5 kpc, taking the inner 80 kpc of the cluster as the extent of the cDs — see below. After correction for an excess of central, young stars (section 3.2) the absolute magnitudes of the cDs are $M_B \sim$ -23. Extrapolating the observational "Kormendy relation" (Kormendy 1977) such bright cDs have $R_{eff} \sim 20h^{-1}$ kpc. Part of this discrepancy is due to an excess of central, young stars, as we shall discuss in section 3.2. We also note that in a study of the formation of the brightest cluster galaxy (BCG) based on a pure N-body simulation (but of higher resolution than ours) Dubinski (1998) found an effective radius of $\sim$20 kpc for the central BCG.

3.1 Identifying Cluster Galaxies and Intracluster Stars

The first step in identifying the IC stars is to find all galaxies in the clusters. To this end we proceed in the following simple way: by visual inspection of the z=0 frames the stars in all galaxies except the cD are located within 10-15 kpc from the centers of the galaxies. Guided by this typical size of the individual cluster galaxies, a cubic grid of cube-length Δl=10 kpc is overlaid the cluster, and all cubes containing at least $N_{\rm th}$=2 stars are identified. Subsequently, each selected cube is embedded in a larger cube of cube-length $3\Delta l$. If this larger cube contains at least $N_{\rm min}$=7 star particles, which are gravitationally bound by its content of gas, stars and dark matter the system is identified as a potential galaxy. Since the method can return several, almost identical versions of the same galaxy only the one containing the largest number of star particles is kept and classified as a galaxy. We tested the galaxy identification algorithm by varying Δl, $N_{\rm th}$, $N_{\rm min}$, and also the numerical resolution of the simulations (section 3.7) and found it to be adequately robust for the purposes of this paper.

The algorithm identifies $N_{\rm gal}$=42 and 94 galaxies inside of the virial radii of C1 and C2, respectively, plus a cD at the center of each cluster. The ratio $N_{\rm gal}$(C2)/$N_{\rm gal}$(C1) is smaller than the ratio of the corresponding virial masses due to the baryonic under-sampling in cluster C2, as discussed above. Apart from the cD there are no galaxies inside of $r_{\rm cD}$=80 kpc in either of the z=0 frames (this is not true in all $z \sim$0 frames for clusters C1 and C2, though, but we tested that the results we present in the following did not depend on which $z \sim$0 frame was chosen to represent the present epoch — see also below).

We define the system of IC stars as the stars located at cluster-centric distances $r_{\rm cD} \leq r \leq r_{\rm vir}$ and *not* inside of the tidal radius of any galaxy in the cluster. The tidal radius for each galaxy is taken to be the Jacobi limit

$$r_J = \left(\frac{m}{3M}\right)^{1/3} D \quad , \qquad (1)$$

where m is the mass of stars, gas and dark matter in the galaxy (inside of r_J), D is the distance from the cluster center to the galaxy and M is the total mass of the cluster inside of D (e.g., Binney & Tremaine 1987). The cD itself is effectively just the inward continuation of the system of IC stars and the division between IC stars and cD is somewhat arbitrary (we hence below quote intracluster star fractions for $r_{\rm cD}$=80 as well as 40 kpc). The above definition of IC stars is conservative, since we calculate the tidal radii on the basis of the z=0 frame cluster-centric distances of the galaxies. For any galaxy which has been through at least one peri-center passage, this tidal radius should be taken as a firm upper limit. Moreover, some IC stars will be inside of the tidal radius of one of the cluster galaxies just by chance. As the total "tidal volume" of all the cluster galaxies is found to be a few tenth of a percent of the virial volume of the cluster this effect can be neglected, however.

3.2 The Intracluster Star Fraction

Using the above definition we find that the intracluster stars constitute 21 and 28% of the stellar mass inside of the virial radius for clusters C1 and C2, respectively (adopting $r_{\rm cD}$=40 kpc these numbers increase slightly to 28 and 34%). For comparison with observations it is more relevant to look at stellar luminosities. Since ages and metallicities are available for all star particles, the photometric properties are straightforward to calculate treating each star particle as a Single Stellar Population (SSP; see Paper II for details). SSP luminosities are computed by mass-weighted integration of the Padova isochrones (Girardi et al. 2002), according to the Arimoto-Yoshii IMF. We find that the IC stars contribute only 9 and 11% of the cluster B-band luminosities for C1 and C2 respectively. This is significantly less than the observational estimate of $L_{\rm B,IC}/L_{\rm B,tot} \gtrsim 0.2$ (e.g., Arnaboldi 2004). The likely reason for this discrepancy is an excess of stars formed fairly recently at the center of the cD and dominating the B-band luminosity: After a period of major merging at $z \sim$1-2 strong, quasi-stationary cooling flows develop at the centers of the clusters despite the strong, super-nova

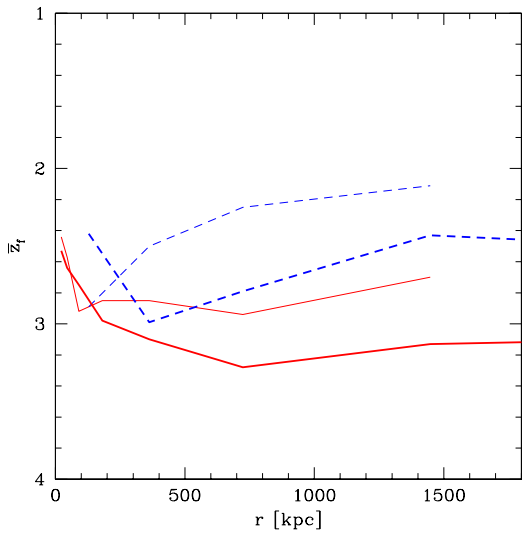

Figure 1. Mean redshift of formation of the cD + IC stars (solid lines) and stars in galaxies (dashed lines) at z=0. Results for cluster C1 ("Virgo-like") are shown by thin lines and for C2 ("mini-Coma") by heavy lines. Statistical uncertainties are $\Delta\bar{z}_f \lesssim 0.05$.

driven energy feedback to the IGM/ICM through galactic super-winds and the use of a fairly top-heavy IMF. As a consequence, stars continue to form steadily at the centers of the cDs ($r \lesssim 10$ kpc) at rates of ∼350 and ∼600 $M_\odot$/yr at z=0 for C1 and C2, respectively. At z=0 the cDs are too blue compared to observed cDs with central B-R colours of ∼1.0 (see Fig. 4) rather than 1.4-1.5 (note though that some star-formation is observed in many cDs at the base of the cooling flow — e.g., McNamara 2004). To make a (albeit crude) correction for this excess of young stars at the centers of the simulated cDs we temporarily discard the luminosity contribution of all stars in the inner r_c=10 kpc with formation redshifts $z_f < z_c$, where z_c is determined by requiring that the mean formation redshift of the remaining stars inside of r_c should be similar to the mean formation redshift of stars at $r \gtrsim r_c$. We find that this is the case for z_c ∼1 and shall in the following in various cases present results with and without this crude correction, adopting z_c=1 for the former. With this correction $L_{\rm B,IC}/L_{\rm B,tot}$=0.29 and 0.42 for the two clusters in better agreement with observations (for $r_{\rm cD}$=40 kpc we obtain $L_{\rm B,IC}/L_{\rm B,tot}$=0.42 and 0.50, respectively), though somewhat high compared to the values found by Feldmeier et al. (2004a) for non-cD clusters. Moreover, the effective radii of the cDs increase to 9 and 11 kpc, respectively. These values are in better agreement with observations (Kormendy 1977) and the finding of Dubinski (1998), but still somewhat smaller. Part of this remaining discrepancy may be due to the effect of gravitational "pinching" of our cDs by the excess, young central stars.

Regarding the intracluster star fraction we show in Paper II that clusters C1 and C2 are deficient in bright galaxies apart from the cDs. As discussed in Paper II, this is probably related to the fact that C1 and C2 are fairly relaxed systems, for which the last major merger took place at $z \gtrsim 1$. Hence it is possible that the galaxies in these clusters suffered more tidal stripping and merging than in an average cluster. To be conservative the above IC star fractions should then be considered upper limits to what would be found for a statistically representative sample of cluster merging histories. Finally, we note that the observed IC star fraction of ∼20% has also been reproduced in the simulations of Murante et al. (2004) and Willman et al. (2004).

3.3 Mean Formation Redshifts, Surface Brightness Profiles and Colours of the Intracluster Stars

In Figure 1 we show the mean (spherically averaged) redshift of formation, $\bar{z}_f$, of the cD + IC stars (solid lines) and stars in galaxies except the cD (dashed lines) as a function of radial distance from the center of the cD for clusters C1 and C2, respectively. For both clusters the average formation redshift of the IC stars is $\bar{z}_{f,IC}$ ∼3 at $r \gtrsim$ 100-200 kpc. The stars in galaxies (except the cD) are on average somewhat younger with $\bar{z}_{f,gal}$ ∼2.5. This is to be expected, since the bulk of the IC stars originate in (proto) galaxies, which have been partly or fully disrupted through tidal stripping in the main cluster potential or by galaxy-galaxy interactions. In contrast, the galaxies still remaining at z=0 have potentially been able to continue forming stars out of remaining cold gas or gas recycled by evolved stars and subsequently cooled to star-forming temperatures and densities. Still, due to ram-pressure stripping of the hot and dilute gas reservoir in galactic haloes and other effects, the star-formation rate in the galaxies decreases significantly from z=2 to 0, considerably more so than in field galaxies cf. Paper II. Murante et al. (2004) find a similar trend that the IC stars are on average older than the stars still in cluster galaxies, but they find somewhat lower mean redshifts of formation, $\bar{z}_f$=1.9 and 1.7 respectively. The reason for this discrepancy is not clear: it may be related to different galactic super-wind prescriptions or that we incorporate metal-dependent radiative cooling in the simulations, whereas Borgani et al. (2004) use a primordial cooling function, but is probably not due to numerical resolution differences (Murante 2004, private communication).

From Figure 1 it can be seen that both IC stars and galactic stars in cluster C2 are on average somewhat older than those in C1. The reason for this is numerical, rather than physical, related to the under-sampling of baryons in the outskirts of the virial volume of the cluster discussed at the beginning of this section: the late infall of gas and galaxies onto the cluster is reduced with respect to a simulation with full baryonic sampling of also the outer parts of the virial volume.

In Figure 2 we show for cluster C2 the azimuthally averaged UBVRIJK surface brightness profiles of the cD+IC stars, both with and without the correction for central, young cD stars discussed above (the H-band results are omitted for clarity). The orientation is such that the cD is viewed along the minor axis, but other orientations give very similar results. The light profiles are approximately described by $r^{1/4}$ laws. In reality the slope flattens with increasing r, so the system can be seen as a central dominant elliptical galaxy surrounded by an extended envelope, with

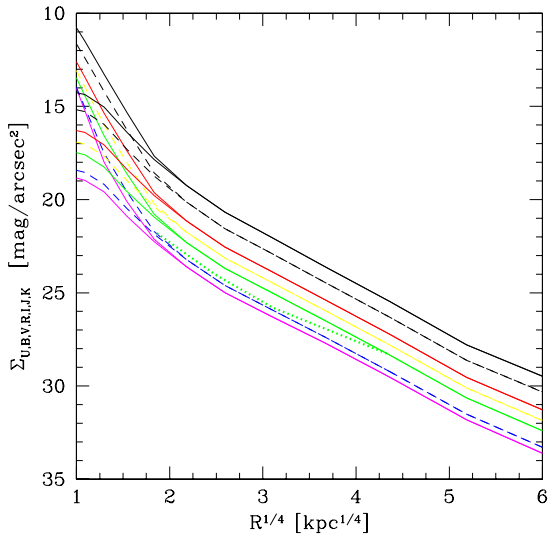

Figure 2. Multiband (UBVRIJK going bottom up) surface brightness profiles of cD + IC stars for cluster C2, shown with (thin lines) and without (thicker lines) the correction for the excess young, central stars, discussed in the text. Also shown (thick dotted line) is V-band surface photometry for the cD in the rich cluster A1413 ($T \simeq$8 keV) obtained by Feldmeier et al. 2002

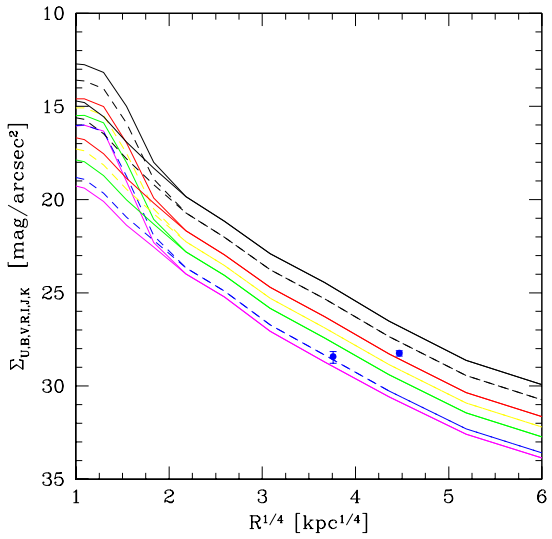

Figure 3. Same as in Figure 2, but now for cluster C1. Data points are B-band IC star estimates based on planetary nebulae observations in the Virgo cluster by Arnaboldi et al. 2002

the slope of the surface brightness profile becoming close to constant beyond $r \sim$40 kpc. These are characteristics of observed cD galaxies (e.g., Feldmeier et al. 2002). Observationally, cD+IC stars can be traced by surface photometry to $V_{lim} \simeq$28.3 mag/arcsec^2 (e.g., Feldmeier et al. 2002), which for cluster C2 corresponds to $r \sim$350 kpc. In Figure 2 we also show V band surface photometry of the cD + envelope in the rich cluster A1413 ($T \simeq$8 keV) obtained by Feldmeier et al. (2002). Though the observational V band profile is slightly flatter than what we predict for the V band, overall agreement is quite good, especially when it is taken into account that the sampling of the baryons becomes increasingly incomplete with radius in cluster C2 (see above). In Figure 3 we show the surface brightness profiles of C1 ("Virgo"). Also shown is two B-band data points derived for Virgo IC stars (indirectly) using planetary nebulae by Arnaboldi et al. (2002). Our predicted B-band profile fits the inner point well, but not the outer one, which is too high (in fact slightly higher than the inner one). The Virgo cluster is known, however, to have an unusually flat galaxy surface brightness profile and possibly be dynamically unrelaxed (Binggeli et al. 1987).

Shown in Figure 4 are the azimuthally averaged B-V, B-R and I-K colours of the cD+IC stars, again with and without the correction discussed above. At about 10 kpc the colours (e.g., $B-V \sim$0.90-0.95) are typical of the stellar populations in the inner parts of cDs (e.g., Mackie 1992). Within 10 kpc this is also the case when correcting for the excess of central, young stars — if not, the core of the cD gets too blue with central colours approaching those of spiral galaxies. Outside of 10 kpc the colour of the cD+IC stars gets bluer with increasing R, but the gradient is very shal-

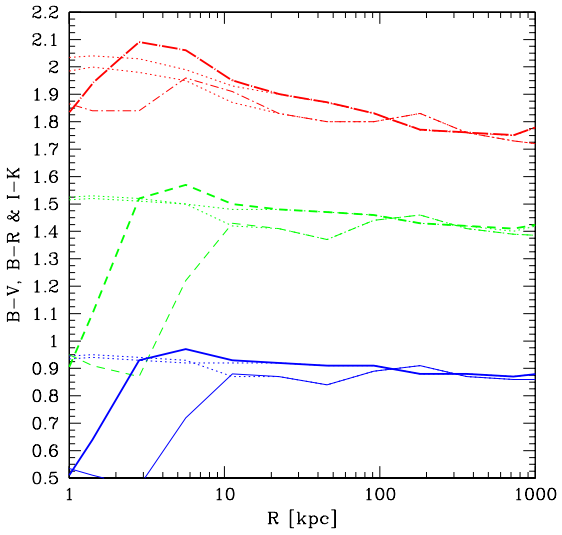

Figure 4. Azimuthally averaged B-V (solid lines), B-R (dashed lines) and I-K (dot-dashed lines) colours of cD + IC stars for clusters C2 (thick lines) and C1 (thinner lines), respectively. The results of applying the correction for the excess, central young stars is shown with thin dotted lines.

low: Δ(B-V) per kpc of $\sim$ -0.0003 As the mean age of the stars is approximately constant with R (see Fig. 1), this is mainly due to a decrease in metal abundance with R (see below). At 100 kpc $B-R \simeq$1.45, typical of sub-L^* E and S0 galaxies (e.g., Gladders et al. 1998). We shall discuss this in a forthcoming paper, but note that cDs are found in general

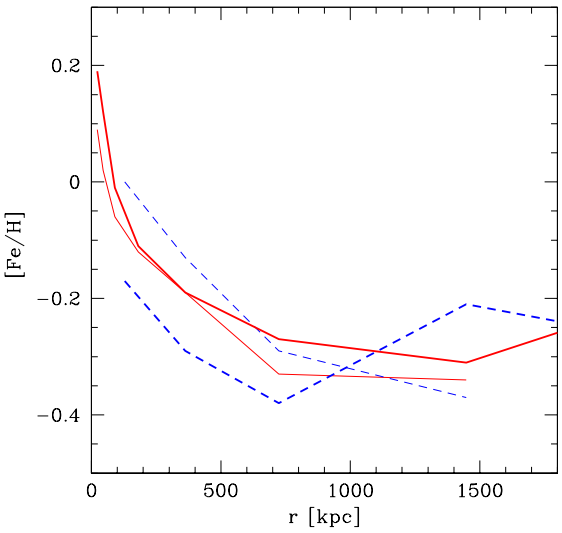

Figure 5. Spherically averaged iron abundance of cD+IC stars (solid lines) and stars in cluster galaxies (dashed lines) for clusters C1 (thin lines) and C2 (thick lines), respectively (results for r <20 kpc are not shown for clarity).

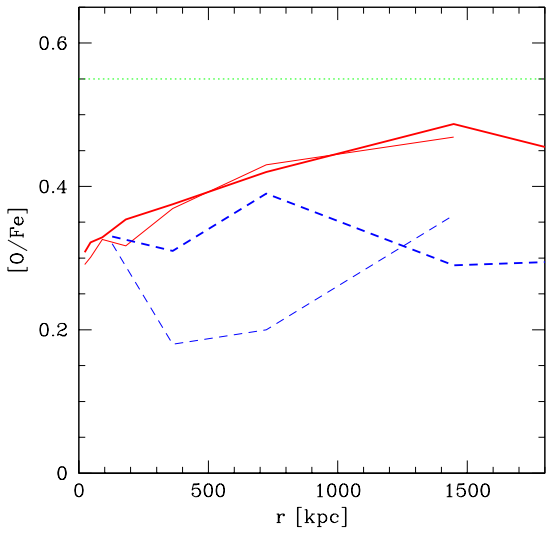

Figure 6. Spherically averaged oxygen-to-iron abundance ratio of cD+IC stars (solid lines) and stars in cluster galaxies (dashed lines) for clusters C1 (thin lines) and C2 (thick lines), respectively. The limiting case for pure SNII enrichment [O/Fe]=0.55 is shown by the thin, dotted line (results for r <20 kpc are not shown for clarity).

to have quite flat colour profiles, in some cases getting redder with R (e.g., Mackie 1992; Garilli et al. 1997; Gonzalez et al. 2000).

3.4 Abundance Properties of the Intracluster Stars and Cluster Galaxies

In Figure 5 we show the spherically averaged iron abundance of the cD+IC stars as well as of the stars in cluster galaxies as a function of cluster-centric distance. Iron is super-solar in the cD+IC stars at $r \lesssim 100$ kpc and decreases to about half solar at large r; the stars in cluster galaxies follow a similar trend. The fairly large overall iron abundance of the IC stars, as compared to, e.g., stars in the halo of the Milky Way, reflects that it is the galaxies (past and present) which have to enrich the 5-10 times more massive hot intracluster medium (ICM) to an iron abundance of about 1/3 solar (Paper I). Durrell et al. (2002) carried out HST observations of an IC field in the Virgo cluster at an average projected distance of 150 kpc from M87 (which for the purposes here can be assumed coincident with cluster center). They confirm an excess of red number counts, which they interpret as IC RGB stars. By comparison with observations of a dwarf irregular, they conclude that these stars have -0.8<[Fe/H]<-0.2. Though this is somewhat less than we predict at r ∼150 kpc, the discrepancy is only a factor of about two, and the observational abundances are clearly significantly larger than those of the halo stars of the Milky Way.

Figure 6 shows the corresponding oxygen-to-iron ratios as a function of r. [O/Fe] is super-solar everywhere. This is in agreement with present estimates for the luminous elliptical galaxies that contain most of the stellar mass in cluster galaxies. For the IC stars no observational information is currently available (Arnaboldi 2004, private communication).

For pure type II supernovae enrichment and with the Arimoto-Yoshii IMF, one expects $[O/Fe]_{SNII}$=0.55 (e.g., Lia, Portinari & Carraro 2002a), so it follows from Fig. 6 that SNe Ia do contribute somewhat to the enrichment of the cD+IC stellar populations, and (not surprisingly) even more so for the stars still in galaxies at z=0 (in fact for an Arimoto-Yoshii IMF the global ($t \rightarrow \infty$) value of the SNII+SNIa enrichment is [O/Fe]=0.18).

3.5 Kinematics of the Intracluster Stars and Cluster Galaxies

Using observed velocities of planetary nebulae it will ultimately be possible to kinematically "dissect" the systems of cD+IC stars in nearby galaxy clusters, such as Virgo. It is hence of considerable interest to determine for our simulations the velocity distribution of the cD+IC stars and compare it to that of cluster galaxies. To this end we proceed as follows: At z=0 cluster C1 and the cD at the center are somewhat flattened (ellipticity $\epsilon = 1 - b/a \simeq 0.4$) with similar minor axis orientations (we shall denote the minor axis of the cD the "z-axis" in the following). Cluster C2 is only slightly flattened ($\epsilon \simeq 0.2$), and so is the cD at the center, with approximately perpendicular minor axis orientations. For each cD+IC star and each cluster galaxy we determine three perpendicular velocity components: The radial component $v_r = \vec{v} \cdot \vec{e}_r$, where $\vec{e}_r$ is the unit vector pointing radially away from the center of the cluster, the perpendicular (tangential) component $v_\phi = \vec{v} \cdot \vec{e}_\phi$, where $\vec{e}_\phi$ is the unit vector perpendicular to $\vec{e}_r$ and aligned with the x-y plane and the

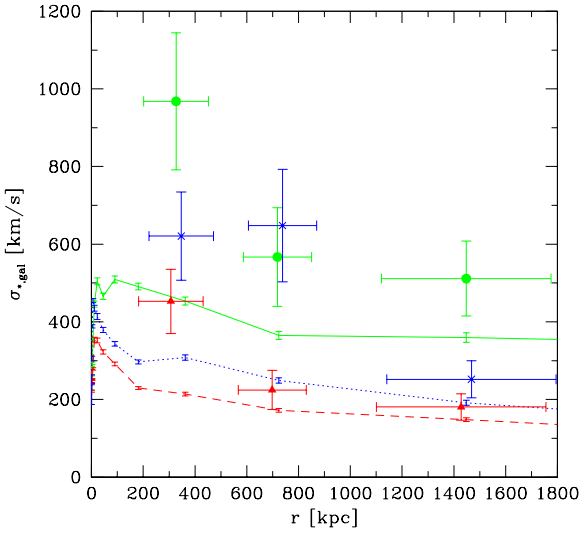

Figure 7. For cD+IC stars in cluster C1 we show the velocity dispersions σ_r (solid lines), σ_ϕ (dotted line) and σ_θ (dashed line). The statistical uncertainties are marked with small errorbars. The similar quantities are shown for the cluster galaxies by filled circles, crosses and filled triangles, with larger errorbars marking the statistical uncertainties.

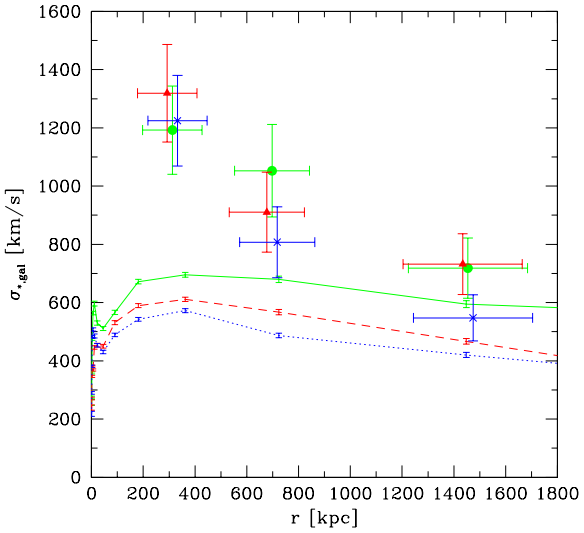

Figure 8. Same as Figure 7, but for cluster C2.

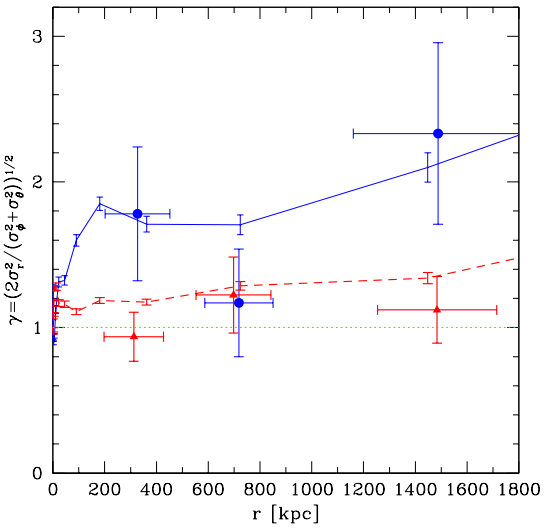

Figure 9. Velocity anisotropy parameter γ for cD+IC stars (solid line) and galaxies (solid circles) for cluster C1. The same is shown for cluster C2 by dashed line and solid triangles. An isotropic velocity distribution has γ=1 indicated by a thin, dotted line.

third (tangential) component v_θ=$\vec{v}\cdot\vec{e}_\theta$, where $\vec{e}_\theta$ is the unit vector $\vec{e}_\theta = \vec{e}_r \times \vec{e}_\phi$.

We calculate the mean rotation $\bar{v}_\phi$ and velocity dispersions σ_r, σ_ϕ and σ_θ of cD+IC stars and galaxies in spherical shells. Outside r ∼10 kpc rotation is found to be dynamically insignificant with $\bar{v}_\phi \lesssim$ 20-40 km/s in both clusters. When correcting for the excess young, central stars rotation is found to be also dynamically unimportant at r <10 kpc. In Figures 7 and 8 we show the velocity dispersions of the cD+IC stars and cluster galaxies in clusters C1 and C2, respectively, versus cluster-centric distance. The cD+IC stars are kinematically significantly colder than the cluster galaxies: The velocity dispersions of the cD+IC stars are in the inner parts of the clusters (r ∼100-500 kpc) only about half of those of the cluster galaxies, increasing slightly to about 70% at r ∼1-2 Mpc. As stars and galaxies are moving in the same gravitational potential this implies by Jean's theorem (e.g., Binney & Tremaine 1987) that the (number) density distribution of cluster galaxies is significantly flatter than that of cD+IC stars, in particular in the inner parts of the clusters — see below. Willman et al. (2004) also find that the IC stars are kinematically colder than the cluster galaxies, except for the innermost part of the cluster. The difference here is probably due to the different definitions of IC stars used: Willman et al. (2004) require the IC stars to be unbound from the "cD" also — this results in large IC star velocity dispersions in the inner parts of the cluster.

The velocity distribution of the cD+IC stars in cluster C1 is highly radially anisotropic at $r \gtrsim 100$ kpc, and, within the statistical uncertainties, this is also the case for the cluster galaxies. We quantify this in Figure 9, where we show $\gamma = \sqrt{(2\sigma_r^2/(\sigma_\phi^2+\sigma_\theta^2))}$, where γ^2 is the ratio of the kinetic energy in radial and mean tangential (1D) motions, respectively. For an isotropic velocity distribution γ=1. In cluster C1 there is almost twice as much kinetic energy in the radial direction than in the sum of the two tangential directions at $r \gtrsim 100$ kpc. Interestingly, within the statistical uncertainties the same appears to hold for the galaxies, which at first seems surprising, since one would expect that it is predominantly galaxies on radial orbits which are tidally disrupted and transformed into cD+IC stars. The explanation for this

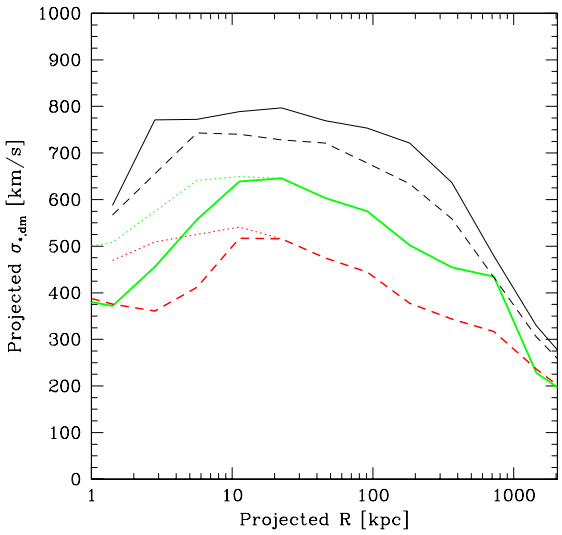

Figure 10. Projected velocity dispersions for cluster C1 of cD+IC stars (thick lines) and dark matter (thinner lines) along the minor axis (z-axis; dashed lines) and averaged along the x and y-axis (solid lines) of the cD/cluster. Thin dotted lines mark the effect of making the correction for the excess young central stars. Statistical uncertainties are $\Delta\sigma \lesssim 20$ km/s.

lack of difference in the orbital characteristics of the two populations is likely the combined effect of radial infall of and dynamical friction on cluster galaxies, but we defer a detailed discussion of this to a forthcoming paper. We note that Willman et al. (2004) find the velocity distribution of the IC stars to be more radially anisotropic than that of the galaxies in the outer parts of their simulated cluster. In cluster C2 the velocity distribution of the cD+IC stars is only mildly radially anisotropic and the velocity distribution of the cluster galaxies is, within the statistical uncertainties, isotropic. We also note that Sommer-Larsen et al. (1997) found that the velocity distribution of Galactic halo stars becomes tangentially anisotropic in the outer halo — the differences probably relate to different accretion kinematics during the build-up of the various haloes — this will also be discussed in a forthcoming paper.

Finally, concerning the flattening of the systems for cluster C1 σ_ϕ is about 50% larger than σ_θ for cD+IC stars as well as galaxies, indicating that these systems are flattened by anisotropic velocity distributions — see below. For cluster C2 $\sigma_\phi \simeq \sigma_\theta$, consistent with this cluster being only mildly flattened.

Observationally, for the cD+IC stars one will only be able to determine line-of-sight velocities using planetary nebulae, not full 3D velocities. For direct comparison with observations we show in Figure 10 the projected velocity dispersions of the cD+IC stars and (for comparison) of the dark matter in cluster C1 versus projected distance from the center of the cD. By dashed lines we show the azimuthally averaged velocity dispersions along the minor axis of the cD. The projected stellar velocity dispersion is 350-400 km/s at the center of the cD, increases to ∼500 km/s at R ∼10-30 kpc and then decreases gradually with increasing R to about 300 km/s at $R_{\rm vir}$. An increase of the stellar velocity dispersion with R has been observed in some cDs, such as A2029 (Dressler 1979), and has been interpreted as marking the transition from galactic to intracluster stars. The effect is less pronounced after correction for the excess young central stars, but we note that these stars still contribute to the gravitational potential and therefore boost the central velocity dispersions. The projected velocity dispersion of the dark matter follows a similar trend with R as that of the stars, but is significantly larger. As the stars and dark matter are moving in the same gravitational potential this implies that the density distribution of dark matter is significantly flatter than that of the cD+IC stars — see below.

The projected velocity dispersions along the major axis of the cD are shown by solid lines. They have been calculated as the average of the projected velocity dispersions along the x-axis and y-axis. Along the x-axis the velocity dispersions are calculated for stars and dark matter particles projecting onto ±30 deg. wedges along the positive and negative y directions, and vice versa for dispersions along the y-axis. The major axis velocity dispersions follow similar trends as the minor axis ones. However, for the cD+IC stars it is significantly larger and for the dark matter halo somewhat larger than along the minor axis. This shows that both systems are flattened by anisotropic velocity dispersions and, as stated above, oriented in similar ways. For cluster C2 the findings are similar (not shown) though the cD is not aligned with the cluster in this case and both systems are only mildly flattened.

Summarizing our findings for the Virgo-like cluster, the typical projected velocity dispersion for the cD+IC stars at $R \gtrsim 50$ kpc is 300-600 km/s depending on orientation and projected distance from the cluster center. Freeman et al. (2000) find a (projected) velocity dispersion of 752±110 km/s for 23 IC planetary nebulae in the Virgo-cluster at a projected distance of about 150 kpc from M87. This value is somewhat larger than our prediction, but it may be due to the "real" Virgo-cluster being kinematically unrelaxed (see also section 3.3); the observational sample is too small to test for velocity substructure (Freeman 2004, private communication).

Since clusters are dynamically fairly young it is important to establish that the results on kinematics etc. are robust, i.e. they do not depend on the particular frame chosen for the analysis. To this end we analyzed for each cluster two frames 1.5 and 3 Gyr before the present time, corresponding to redshifts 0.12 and 0.26, respectively. We find that none of the results presented in this paper change in any significant way when going to these earlier frames.

3.6 Density Distributions of the Intracluster Stars, Cluster Galaxies and the Dark Matter

In Figure 11 we show for cluster C1 the spherically averaged density distributions of the cD+IC stars (with and without the correction for the excess, young central stars), the stars in cluster galaxies, the dark matter and, with an arbitrary normalization, the *number* density of cluster galaxies. As suggested previously, the number density profile of cluster galaxies in the inner parts of the cluster as well as the dark matter density profile in general are significantly flatter than

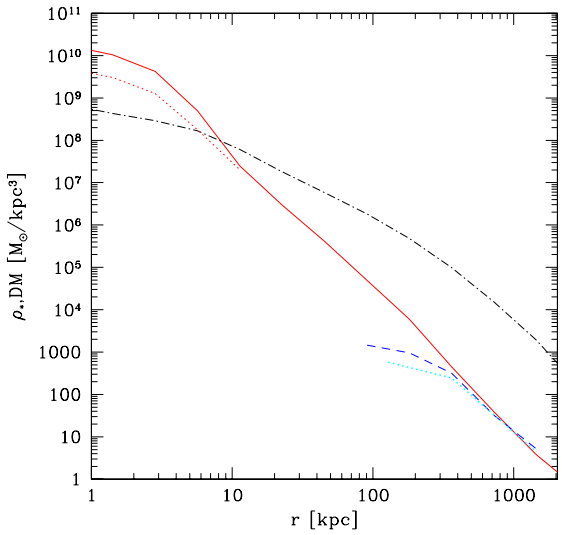

Figure 11. Spherically averaged density profiles for cluster C1 of cD+IC stars (solid line), dark matter (dot-dashed line), stars in cluster galaxies (dashed line) and, with arbitrary normalization, *number* density of cluster galaxies (dotted line). The result of applying the correction for the excess, young central stars is shown by the thin, dotted line.

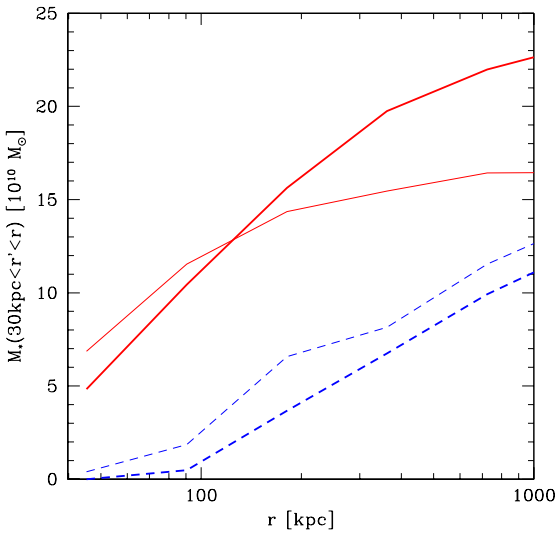

Figure 12. For a $M_{\rm vir}$=3.4x10^{13} h^{-1}M$_\odot$ (T=1.1 keV) group is shown at z=0.1 the cumulative mass in cD+IC stars (solid lines) and in stars in cluster galaxies (dashed lines) outside of r=30 kpc for the normal resolution (thin lines) and high resolution (thick lines) simulations, respectively.

the density profile of cD+IC stars. For the cluster galaxies this is a manifestation of the transformation of galaxies to cD+IC stars by tidal disruption in the inner parts of the cluster.

Moreover, it follows from Fig.11 that the average (mass) density of stars in cluster galaxies only exceeds that of the IC stars beyond about half the virial radius - this is in good agreement with the findings of Murante et al. (2004).

3.7 A Numerical Resolution Test

It is important to test whether the properties of the IC star population presented in this paper depend much on the numerical resolution of the simulations. In the present paper, we address resolution effects by discussing a smaller system, a group of virial mass $3.4 \times 10^{13} h^{-1} M_\odot$ and emission–weighted temperature 1.1 keV. The group was run at the same "standard" resolution as clusters C1 and C2, as well as with eight times higher mass and two times higher force resolution. This results in particle masses of $m_{\rm gas}$=m_*=3.1x10^7 and $m_{\rm DM}$=2.3x10^8 h^{-1}M$_\odot$ and gravity softening lengths of 1.4, 1.4 and 2.7 h^{-1}kpc, respectively. In order to enable an optimal comparison between the normal and high resolution runs only Fourier modes up the Nyquist wavenumber of the normal resolution simulation were used to prepare the initial conditions for the high resolution run (i.e., additional high-wavenumber modes up to the Nyquist wavenumber of the high resolution simulation were *not* added to the Fourier modes).

The resulting group looks like a "scaled down" version of clusters C1 and C2. In particular, it has a prominent central galaxy, which we denote as the "cD", like in the cluster simulations — in this respect it is similar to the so-called "fossil" groups (e.g., Jones et al. 2003).

In Figure 12 we show the cumulative mass of cD+IC stars and stars in galaxies outside of r=30 kpc for the normal and high resolution runs at z=0.1 (at z=0 one large group galaxy is merging with the cD). There is reasonable agreement between the runs — the somewhat larger mass in IC stars in the high resolution simulation at $r \gtrsim$200-300 kpc is likely due to the better resolution of star-forming gas in the lower over-density regions which come to populate the outer parts of the group.

As one goes to higher resolution one might naively expect that the fraction of IC stars in the simulations decreases as the cluster galaxies are increasingly well resolved. The interesting indication from Figure 12 is, however, that if anything the fraction of IC stars slightly *increases* with increasing numerical resolution.

Shown in Figure 13 at z=0.1 are the azimuthally averaged velocity dispersions of cD+IC stars and dark matter projected along the minor axis of the cD for the normal and high resolution simulations, and with the correction for excess young central stars discussed previously applied. The agreement is overall reasonable, especially when it is taken into account that there are at z=0.1 just 1235 cD+IC stars inside of the virial radius in the normal resolution simulation of this group. This is a factor 10-20 less than the corresponding numbers for clusters C1 and C2. The increase in central velocity dispersion ($R \lesssim$10 kpc) for the high resolution simulation, in particular for the stars, is likely an effect of the increased force resolution. Note also the qualitative similarity between the velocity dispersion profiles shown in Fig. 13, and the results for cluster C1 (Fig. 10).

Finally, as a test of resolution dependence of chemical

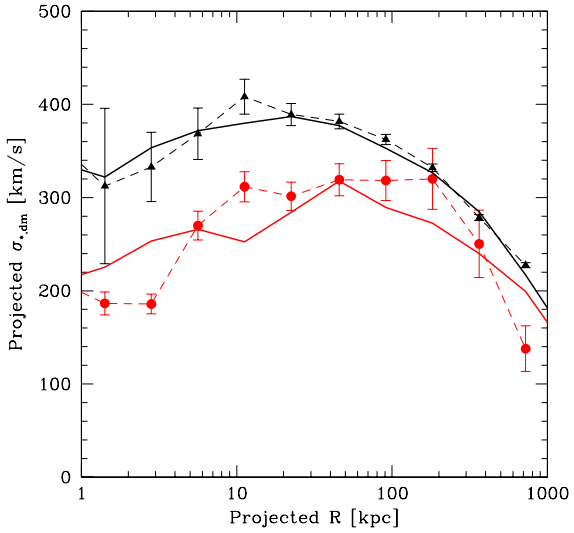

Figure 13. Velocity dispersions projected along the minor axis of the "cD" for the cD+IC stars (lower curves and symbols) and dark matter (upper curves and symbols) in the group. Results for the normal resolution simulation are connected by dashed lines and are shown as solid circles with errorbars (stars) and solid triangles with errorbars (dark matter). Results for the high resolution simulation are shown by solid lines.

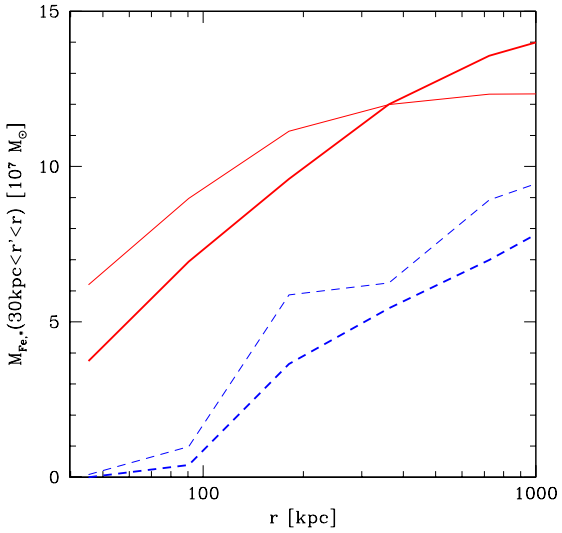

Figure 14. Same as Figure 12, except that cumulative masses of Iron are shown.

evolution and metal abundances we show in Figure 14 the cumulative mass of Iron in cD+IC stars and stars in galaxies outside of r=30 kpc for the normal and high resolution runs. There is reasonable agreement between the runs and we note that in relation to Figure 12 this is a nontrivial result, since a significant fraction of the iron produced by the stars ends up in the hot ICM (Paper I).

In general, as mentioned at the beginning of section 3, we carry out all the analysis of the (normal resolution) cluster simulations C1 and C2 presented in this paper for the normal and high resolution group simulations also. On this basis we find that all results given in this paper appear largely robust to resolution changes. Ultimately, however, this can only be properly checked by running the "production" simulations C1 and C2 at higher numerical resolution. To this end we have initiated a high resolution simulation of C1 (with similar numerical characteristics as the above high-resolution group simulation) — at z=1.3 we find no significant differences between the "standard" and high-resolution simulations of C1 in relation to the results presented in this paper.

4 CONCLUSIONS

In this paper we have discussed the properties of the intracluster (IC) stellar populations. Our results are based on cosmological simulations of galaxy clusters including self-consistently metal-dependent atomic radiative cooling, star-formation, supernova driven galactic super-winds, non-instantaneous chemical evolution and the effects of a meta-galactic, redshift dependent UV field. In relation to modelling the properties of the IC stars this is an important step forward with respect to previous theoretical works on the subject which were based on purely N-body (collisionless) simulations, apart from the recent, interesting work by Murante et al. (2004).

The main results from our simulations of a Virgo-like (C1) and a (sub) Coma-like (C2) galaxy cluster regarding the IC stellar populations are as follows:

The intracluster (IC) stars are found to contribute 20-40% of the total cluster B-band luminosity at z=0 and to form at a mean redshift $\bar{z}_f$ ∼3, somewhat larger than the mean formation redshift of the stars in cluster galaxies which is about 2.5. This difference corresponds to a time span of about 0.5 Gyr. Murante et al. (2004) find somewhat lower mean formation redshifts of 1.9 and 1.7, respectively — the reason for this discrepancy between the two works remains to be identified.

We calculate UBVRIJHK surface brightness profiles of the IC star populations and find that the profile of the larger cluster matches the observed V-band profile of Abell 1413 (T ≃8 keV) quite well. For the Virgo-like cluster we fail, however, to match the flat profile between 200 and 400 kpc projected cluster-centric distance observationally (but indirectly) inferred for the Virgo cluster by Arnaboldi et al. (2002) from planetary nebulae counts. We note though that the galaxy distribution in Virgo is also unusually flat (Binggeli et al. 1987). The V-band surface brightness is found to reach V_{lim} ≃28.3 mag/arcsec^2 (Feldmeier et al. 2002) in cluster C2 at r ∼350 kpc and in cluster C1 at r ∼250 kpc. The typical colour of the IC stellar population is B-R=1.4-1.5, comparable to the colour of sub-L^* E and S0 galaxies. The mean Iron abundance of the IC stars is about solar in the central part of the cluster (r ∼100 kpc) gently decreasing to about half solar at the virial radius. The IC stars are α-element enhanced with, e.g, [O/Fe] increasing

slightly with r and characterized by a typical [O/Fe]$\sim$0.4 dex.

The IC stars are kinematically significantly colder than the cluster galaxies: The velocity dispersions of the IC stars are in the inner parts of the cluster (r $\sim$100-500 kpc) only about half of those of the cluster galaxies increasing slightly to about 70% at r=1-2 Mpc. The typical projected velocity dispersion in the Virgo-like cluster at $R \gtrsim 50$ kpc is 300-600 km/s depending on orientation and projected distance from the cluster center. Rotation is found to be dynamically insignificant for the IC stars. The velocity distributions of IC stars *and* clusters galaxies are in one cluster highly radially anisotropic, in the other close to isotropic.

A test simulation of a $T \simeq$1.1 keV group at higher numerical resolution indicates that the results presented are largely robust to resolution changes. Work is in progress to simulate also at higher resolution the two clusters discussed in this paper. Moreover, we are in the process of enlarging significantly our sample of galaxy clusters.

ACKNOWLEDGEMENTS

We have benefited considerably from discussions with Magda Arnaboldi, John Feldmeier, Ken Freeman, Anthony Gonzalez, Giuseppe Murante and Beth Willman. Moreover, the comments by the anonymous referee significantly improved the presentation of our results.

All computations reported in this paper were performed on the IBM SP4 facility provided by Danish Center for Scientific Computing (DCSC). We gratefully acknowledge the abundant access to computing time on this system. This work was supported by Danmarks Grundforskningsfond through its support for the establishment of the Theoretical Astrophysics Center (TAC), and the Villum Kann Rasmussen Foundation.

REFERENCES

Arnaboldi, M., 2004, IAU Symp., **217**, Recycling intergalactic and interstellar matter, eds. P.-A. Duc, J. Braine, and E. Brinks., p.54
Arnaboldi, M. et al., 2002, AJ, 123, 760
Arnaboldi, M. et al., 2003, AJ, 125, 514
Binggeli, B., Tammann, G.A., & Sandage, A., 1987, AJ, 94, 251
Binney, J., & Tremaine, S. 1987, Galactic Dynamics. Princeton Univ. Press, Princeton
Borgani, S., 2004, MNRAS, 348, 1078
Bryan G.L., Norman M.L., 1998, ApJ 495, 80
Cleary, P. W., & Monaghan, J. J., 1999, Journal of Computational Physics, 148, 227
Dressler, A., 1979, ApJ, 231, 659
Dubinski, J., 1998, ApJ, 502, 141
Dubinski, J., Koranyi, D., & Geller, M., 2003, IAU symposium, 208, 237
Durrell, P.R., Ciardullo, R., Feldmeier, J.J., Jacoby, G.H., & Sigurdsson, S., 2002, ApJ, 570, 119
Ettori, S., & Fabian, A.C., 2000, MNRAS, 317, 57
Feldmeier, J.J., et al., 2002, ApJ, 575, 779
Feldmeier, J.J., et al., 2004a, ApJ, 609, 617
Feldmeier, J.J., Ciardullo, R., Jacoby, G.H., & Durell, P.R., 2004b, ApJ, in press (astro-ph/0407274)
Ferguson, A.M.N., Irwin, M.J., Ibata, R.A., Lewis, G.F., & Tanvir, N.R., 2002, AJ, 124, 1452
Freeman, K.C., et al., 2000, ASP Conf. Series, 197, 389
Gal-Yam, A., et al., 2003, AJ, 125, 1087
Garilli, B., et al., 1997, AJ 113, 1973
Girardi, L., et al., 2002, A&A, 391, 191
Gladders, M.D., et al., 1998, ApJ, 501, 571
Gonzalez, A.H, et al., 2000, ApJ, 536, 561
Gonzalez, A.H, Zabludoff, A.I., & Zaritsky, D. 2004, ApJ, submitted (astro-ph/0406244)
Haardt, F., & Madau, P. 1996, ApJ, 461, 20
Helmi, A., White, S.D.M., de Zeeuw, P.T., & Zhao, H., 1999, Nature, 402, 53
Helmi, A., White, S.D.M., & Springel, V., 2003, MNRAS, 339, 834
Jones, L.R., Ponman, T.J., Horton, A., Babul, A., Ebeling, H. & Burke, D.J., 2003, MNRAS, 343, 627
Kormendy, J., 1977, ApJ, 218, 333
Lia, C., Portinari, L., & Carraro, G. 2002a, MNRAS, 330, 821
Lia, C., Portinari, L., & Carraro, G. 2002b, MNRAS, 335, 864
Lin Y.-T., Mohr J.J., 2004, ApJ in press (astro-ph/0408557)
Mackie, G. 1992, ApJ 400, 65
McNamara, B. R. 2004, in "The Riddle of Cooling Flows in Galaxies and Clusters of Galaxies", Charlottesville, Virginia, USA, Eds. T.H.Ruprecht, J.C.Kempner & N.Soker
Mori, M., Yoshii, Y., Tsujimoto, T., & Nomoto, K. 1997, ApJ, 478, L21
Murante, G., et al., 2004, ApJ, 607, L83
Napolitano, N.R., et al., 2003, ApJ, 594, 172
Oemler, A. Jr., 1976, ApJ, 209, 693
Romeo, A.D., Portinari, L., & Sommer-Larsen, J., 2004, MNRAS, submitted (astro-ph/0404445, Paper II)
Romeo, A.D., Sommer-Larsen, J., Portinari, L., & Antonuccio, V., 2004, MNRAS, in preparation (Paper I).
Sommer-Larsen J., Dolgov A., 2001, ApJ 551, 608
Sommer-Larsen, J., Beers, T.C., Flynn, C., Wilhelm, R., & Christensen, P. R. 1997, ApJ, 481, 775
Sommer-Larsen J., Götz M., Portinari L., 2003, ApJ, 596, 46
Springel, V., & Hernquist, L., 2002, MNRAS, 333, 649
Tornatore, L., Borgani, S., Matteucci, F., Recchi, S., & Tozzi, P., 2004, MNRAS, 349, L19
Valdarnini, R., 2003, MNRAS, 339, 1117
Willman, B., Governato, F., Wadsley, J., & Quinn, T., 2004, MNRAS, submitted (astro-ph/0405094)
Zaritsky, D., Gonzalez, A.H, & Zabludoff, A.I., 2004, ApJ, 613, L93